

Lightest Member of the Basic Carboxylate Structural Pattern:

 $[Al_3(\mu_3-O)(\mu-O_2CCF_3)_6(THF)_3][[(Me_3Si)_3CAI(O_2CCF_3)_3] \cdot C_7H_8$ Hagen Hatop,[†] Marilena Ferbinteanu,^{†,‡} Herbert W. Roesky,^{*,†,||} Fanica Cimpoesu,[§] Marcus Schiefer,[†] Hans-Georg Schmidt,[†] and Mathias Noltemeyer[†]

Institut für Anorganische Chemie der Universität Göttingen, Tammannstrasse 4, D-37077 Göttingen, Germany, and Institute of Physical Chemistry, Splaiul Independentei 202, 77208 Bucharest, Romania

Received August 14, 2001

Introduction

Basic chromium acetate¹ plays an important role in the history of coordination chemistry. Its μ_3 -oxo-trinuclear pattern appears as a distinguished structural prototype of the polynuclear complexes,² being encountered in innumerable systems of Cr,³ Mn,⁴ and Fe⁵ and also with the heavier metals (Ru,⁶ Ir,⁷ W⁸). Various mixed valent species with Mn or Fe are well-known examples for the special magnetic and optical problems related with the localized versus the delocalized

* Author to whom correspondence should be addressed. E-mail: hroesky@gwdg.de.

[†] Institut für Anorganische Chemie der Universität Göttingen.

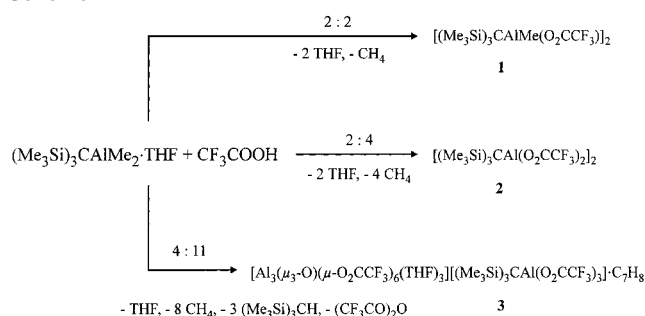
[‡] Permanent address: University of Bucharest, Faculty of Chemistry, Inorganic Chemistry Department, Dumbrava Rosie 23, Bucharest 70254, Romania. E-mail: mcimpoesu@yahoo.com.

[§] Institute of Physical Chemistry.

^{||} Dedicated to Professor Gottfried Huttner on the occasion of his 65th birthday.

- (1) Chang, S. C.; Jeffrey, G. A. *Acta Crystallogr. Sect. B* **1970**, *26*, 673–674.
 (2) (a) Cannon, R. D.; White, R. P. *Prog. Inorg. Chem.* **1988**, *36*, 195–298. (b) Anson, C. E.; Bourke, J. P.; Cannon, R. D.; Jayasooriya, U. A.; Molinier, M.; Powell, A. K. *Inorg. Chem.* **1997**, *36*, 1265–1266.
 (3) (a) Schenk, K. J.; Güdel, H. U. *Inorg. Chem.* **1982**, *21*, 2253–2256. (b) Anson, C. E.; Chai-Saard, N.; Bourke, J. P.; Cannon, R. D.; Jayasooriya, U. A.; Powell, A. K. *Inorg. Chem.* **1993**, *32*, 1502–1507. (c) Bourke, J. P.; Karu, E.; Cannon, R. D. *Inorg. Chem.* **1996**, *35*, 1577–1581. (d) Cannon, R. D.; Jayasooriya, U. A.; Sowrey, F. E.; Tilford, C.; Little, A.; Bourke, J. P.; Rogers, R. D.; Vincent, J. B.; Kearley, G. J. *Inorg. Chem.* **1998**, *37*, 5675–5676. (e) Lieberman, R. L.; Bino, A.; Mirsky, N.; Summers, D. A.; Thompson, R. C. *Inorg. Chim. Acta* **2000**, *297*, 1–5.
 (4) (a) Baikie, A. R. E.; Hursthouse, M. B.; New, L.; Thornton, P.; White, R. G. *J. Chem. Soc., Chem. Commun.* **1980**, 684–685. (b) Ribas, J.; Albela, B.; Stoeckli-Evans, H.; Christou, G. *Inorg. Chem.* **1997**, *36*, 2352–2360. (c) Li, J.; Yang, S. M.; Zhang, F. X.; Tang, Z. X.; Ma, S. L.; Shi, Q. Z.; Wu, Q. J.; Huang, Z. X. *Inorg. Chim. Acta* **1999**, *294*, 109–113.
 (5) Lippard, S. J. *Angew. Chem., Int. Ed. Engl.* **1988**, *27*, 344–361. (b) Wu, G.; Zhang, Y.; Ribaud, L.; Coppens, P.; Wilson, C.; Iversen, B. B.; Larsen, F. K. *Inorg. Chem.* **1998**, *37*, 6078–6083. (c) Jayasooriya, U. A.; Cannon, R. D.; Anson, C. E.; Arapkoske, S. K.; White, R. P.; Kearley, G. J. *J. Chem. Soc., Chem. Commun.* **1992**, 379–381. (d) Fu, D. G.; Wang, G. X.; Tang, W. X. *Polyhedron* **1993**, *12*, 2459–2463.
 (6) (a) Abe, M.; Sasaki, Y.; Yamaguchi, T.; Ito, T. *Bull. Chem. Soc. Jpn.* **1992**, *65*, 1585–1590. (b) Powell, G.; Richens, D. T.; Bino, A. *Inorg. Chim. Acta* **1995**, *232*, 167–170.
 (7) Almog, O.; Bino, A.; Garfinkel-Shweky, D. *Inorg. Chim. Acta* **1993**, *213*, 99–102.
 (8) Ardon, M.; Cotton, F. A.; Dori, Z.; Fang, A.; Kapon, M.; Reisner, G. M.; Shaia, M. *J. Am. Chem. Soc.* **1982**, *104*, 5394–5398.

Scheme 1



character of itinerant electrons.⁹ The μ_3 -oxo-trinuclear prototype appears within a certain variety of ligands, but the carboxylates seem to be the symbiotic companions of the central oxygen, bridging the equatorial positions of the metal ions with the central μ_3 -O atom. The reaction of $(Me_3Si)_3CAI Me_2 \cdot THF$ with one, two, or three equivalents of CF_3COOH yielded $[(Me_3Si)_3CAI Me(O_2CCF_3)_2]_2$ (**1**), $[(Me_3Si)_3CAI(O_2CCF_3)_2]_2$ (**2**), and $[Al_3(\mu_3-O)(\mu-O_2CCF_3)_6(THF)_3][[(Me_3Si)_3CAI(O_2CCF_3)_3] \cdot C_7H_8]$ (**3**), respectively (Scheme 1). The cation $[Al_3(\mu_3-O)(\mu-O_2CCF_3)_6(THF)_3]^+$ of **3** is so far the lightest member of the oxo-centered trinuclear class of complexes, although within the main group metal ions, a gallium analogue is known, $[Ga_3(\mu_3-O)(\mu-O_2CC_6H_5)_6(4-MePy)_3]^+$.¹⁰ Up to now, an Al_3O core was obtained only in asymmetrical patterns,¹¹ involving aza-indole ligands and aluminum centers with different coordination numbers. Compound **3** is the first symmetrical example that confirms a

- (9) (a) Wroblewski, J. T.; Dziobkowski, C. T.; Brown, D. B. *Inorg. Chem.* **1981**, *20*, 684–686. (b) McCusker, J. K.; Jang, H. G.; Wang, S.; Christou, G.; Hendrickson, D. N. *Inorg. Chem.* **1992**, *31*, 1874–1880. (c) Wu, R. W.; Poyraz, M.; Sowrey, F. E.; Anson, C. E.; Wocadlo, S.; Powell, A. K.; Jayasooriya, U. A.; Cannon, R. D.; Nakamoto, T.; Katada, M.; Sano, H. *Inorg. Chem.* **1998**, *37*, 1913–1921. (d) Wilson, C.; Iversen, B. B.; Overgaard, J.; Larsen, F. K.; Wu, G.; Paliu, S. P.; Timco, G. A.; Gerbeleu, N. V. *J. Am. Chem. Soc.* **2000**, *122*, 11370–11379. (e) Wu, C. C.; Hunt, S. A.; Gantzel, P. K.; Gütllich P.; Hendrickson, D. N. *Inorg. Chem.* **1997**, *36*, 4717–4733.
 (10) Andras, M. T.; Duraj, S. A.; Hepp, A. F.; Fanwick, P. E.; Bodnar, M. *J. Am. Chem. Soc.* **1992**, *114*, 786–787.
 (11) (a) Gao, S.; Wu, Q.; Wu, G.; Wang, S. *Organometallics* **1998**, *17*, 4666–4674. (b) Liu, W.; Hassan, A.; Wang, S. *Organometallics* **1997**, *16*, 4257–4259.

long-standing unproved assumption that the basic aluminum acetates, well-known as chemical reagents,¹² possess a structural variety analogous to the chromium one.¹³ The synthesis of **3** by using the organometallic precursor (Me₃Si)₃CAI Me₂·THF offered a valid option for generating basic carboxylates, as compared to the synthesis in water, where probably colloidal hydroxo species are precluding formation of crystal phases.

Experimental Section

General Data. All experiments were carried out using standard Schlenk techniques under a dry nitrogen atmosphere because of the sensitivity of the reactants and products toward air and moisture. A Braun MB 150-GI box was used to store the compounds and to prepare the samples for spectroscopic characterization. All solvents were distilled from sodium/benzophenone and degassed prior to use. (Me₃Si)₃CAI Me₂·THF was prepared as described in the literature.¹⁴ Elemental analyses were performed at the Analytisches Labor des Instituts für Anorganische Chemie der Universität Göttingen. NMR spectra were recorded on a Bruker Avance 200 or Bruker Avance 500 spectrometer, and chemical shifts were referenced to Me₄Si and C₆F₆, respectively. FT-IR spectra were measured on a Bio-Rad FTS-7 as CsI or KBr pellets in the range 4000–400 cm⁻¹. Mass spectra were obtained on Finnigan MAT 8230 and Varian MAT CH 5 instruments by EI- and FAB-MS techniques. Decomposing points were measured in sealed glass tubes on a Büchi 540 instrument.

Synthesis of [(Me₃Si)₃CAI Me(O₂CCF₃)₂]₂ (1). CF₃COOH (0.335 g, 2.94 mmol) was added to a solution of (Me₃Si)₃CAI Me₂·THF (1.06 g, 2.94 mmol) in toluene (20 mL). The cloudy liquid was stirred for 1 day. An insoluble residue was filtered off and recrystallized at -20 °C from THF. Small amounts of adherent solvent were removed in vacuo. Compound **1** (0.42 g, 0.54 mmol, 37%) was obtained as a colorless solid (decomposing at 210 °C). ¹H NMR (200 MHz, THF-*d*₈, ppm): δ -0.47 (s, 3 H, AlCH₃), 0.23 (s, 27 H, SiCH₃). ¹⁹F NMR (188 MHz, THF-*d*₈, ppm): δ -74.7 (s). ²⁹Si NMR (99 MHz, THF-*d*₈, ppm): δ -4.1 (s). MS (EI): *m/z* 757 (30%, M - Me), 371 (100%, M/2 - Me). IR (KBr, cm⁻¹): 2959, 1736, 1700, 1503, 1428, 1261, 1210, 1178, 1050, 851, 724, 673. Anal. Calcd for C₂₆H₆₀Al₂F₆O₄Si₆: C, 40.39; H, 7.82. Found: C, 41.1; H, 7.8.

Synthesis of [(Me₃Si)₃CAI(O₂CCF₃)₂]₂ (2). CF₃COOH (0.860 g, 7.54 mmol) was added to a solution of (Me₃Si)₃CAI Me₂·THF (1.36 g, 3.77 mmol) in toluene (20 mL) and stirred for 1 day. All solvents were removed in vacuo. The remaining solid was treated with *n*-hexane (20 mL) and filtered. Crystallization in toluene at -20 °C afforded **2** (1.66 g, 1.71 mmol, 45%) as a colorless solid (decomposing at 170 °C). ¹H NMR (200 MHz, THF-*d*₈, ppm): δ 0.23 (s). ¹⁹F NMR (188 MHz, THF-*d*₈, ppm): δ -74.8 (s). ²⁹Si NMR (99 MHz, THF-*d*₈, ppm): δ -3.1 (s). MS (EI): *m/z* 953 (100%, M - Me). IR (KBr, cm⁻¹): 2960, 1762, 1749, 1417, 1265, 1217, 1192, 1162, 854, 836, 723, 676. Anal. Calcd for C₂₈H₅₄Al₂F₁₂O₈Si₆: C, 34.70; H, 5.62. Found: C, 35.0; H, 5.7.

Synthesis of [Al₃(μ₃-O)(μ-O₂CCF₃)₆(THF)₃][(Me₃Si)₃CAI(O₂CCF₃)₃·C₇H₈] (3). CF₃COOH (1.99 g, 16.5 mmol) was added to a solution of (Me₃Si)₃CAI Me₂·THF (2.00 g, 5.50 mmol) in toluene (20 mL) and stirred for 1 day. All volatile substances were pumped off. The residue was dissolved in toluene/THF (5:1) and

Table 1. Crystal Data and Structure Refinement for **3**

empirical formula	C ₄₇ H ₅₉ Al ₄ F ₂₇ O ₂₂ Si ₃
fw	1681.13
temp (K)	200(2)
cryst size (mm ³)	1.0 × 0.7 × 0.5
cryst syst	rhombohedral
space group	R $\bar{3}$
<i>a</i> = <i>b</i> = <i>c</i> (Å)	18.313(2)
α = β = γ(deg)	53.472(17)
<i>V</i> (Å ³)	3679.3(7)
<i>Z</i>	2
ρ _{calcd} (g mm ⁻³)	1.517
μ (mm ⁻¹)	0.246
<i>F</i> (000)	1708
2θ range (deg)	7–50
index ranges	-14 ≤ <i>h</i> ≤ 21, -21 ≤ <i>k</i> ≤ 21, -12 ≤ <i>l</i> ≤ 18
reflns collected	4633
independent reflections	4341 (<i>R</i> _{int} = 0.1241)
data/restraints/parameters	4341/599/368
GOF <i>F</i> ²	1.013
<i>R</i> , w <i>R</i> ² (<i>I</i> > 2σ(<i>I</i>))	0.0712, 0.1918
<i>R</i> , w <i>R</i> ² (all data)	0.0889, 0.2112
largest diff peak and hole (e Å ⁻³)	1.284 and -0.698

$$^a R = \sum ||F_o| - |F_c|| / \sum |F_o|. \quad ^b wR2 = [\sum w(F_o^2 - F_c^2)^2] / [\sum w(F_o^2)^2]^{1/2}.$$

crystallized for one week at -20 °C. Compound **3** was obtained in 10% yield (0.18 g, 0.11 mmol) (decomposing at 135 °C). ¹H NMR (200 MHz, THF-*d*₈, ppm): δ 0.26 (s). ¹⁹F NMR (188 MHz, THF-*d*₈, ppm): δ -77.4 (s, 1 F), -75.9 (s, 1 F), -75.8 (s, 1 F). ²⁹Si NMR (99 MHz, THF-*d*₈, ppm): δ -3.0 (s). MS (FAB_{pos}): *m/z* 991 (10%, [M_{cation}⁺]), 919 (100%, [M_{cation}⁺ - THF]). MS (FAB_{neg}): *m/z*, 597 (100%, [M_{anion}⁻]). IR (CsI, cm⁻¹): 2962, 1763, 1735, 1521, 1236, 1179, 1008, 860, 803, 735, 663, 566, 452, 410, 369. Anal. Calcd for C₄₇H₅₉Al₄F₂₇O₂₂Si₃: C, 33.58; H, 3.54. Found: C, 34.3; H, 3.8.

X-ray Structure Determination of 3. A suitable single crystal for an X-ray structural analysis of **3** was obtained from a saturated toluene/THF solution (8:1) at -20 °C. Diffraction data were collected on a Siemens-Stoe AED diffractometer (at -70 °C) with graphite-monochromated Mo Kα radiation (λ = 0.710 73 Å). The structure was solved by direct methods¹⁵ and refined against *F*² on all data by full-matrix least squares with SHELXL-93.¹⁶ All non-hydrogen atoms were refined anisotropically and included at geometrically calculated positions and refined using a riding model. Other details of the data collection, structure solution, and the refinement are listed in Table 1. The crystallographic data reveal a disorder on the CF₃-groups.

Results and Discussion

The stepwise formation of compounds **1–3** can be rationalized as follows: The first step is the exchange of a methyl group at (Me₃Si)₃CAI Me₂·THF by CF₃COO⁻ followed by replacement of the second one by a CF₃COO⁻. Inadvertently present water or water generated from condensation of CF₃COOH in this strongly acidic solution then accounts for the cleavage of the remaining Al–C bonds under formation of the cation. The anion of **3** results from addition of CF₃COO⁻ to **2** (Scheme 1).

According to the numerically computed vibrational spectrum,¹⁸ which identified intense A₂' modes at 643 and 736

(12) Basic aluminum acetates: CASRN 142-03-0.

(13) (a) Spacu, G.; Popper, E. *Kolloid-Z.* **1943**, *103*, 19–21. (b) Starke, K. *J. Inorg. Nucl. Chem.* **1960**, *13*, 254–257.

(14) Schnitter, C.; Roesky, H. W.; Albers, T.; Schmidt, H.-G.; Röpken, C.; Parisini, E.; Sheldrick, G. M. *Chem.—Eur. J.* **1997**, *3*, 1783.

(15) Sheldrick, G. M. *Acta Crystallogr. Sect. A* **1990**, *46*, 467.

(16) Sheldrick, G. M. *SHELXL-93*, Program for Crystal Structure Refinement; University of Göttingen: Göttingen, Germany, 1993.

(17) Pandey, A.; Gupta, V. D.; Nöth, H. *Eur. J. Inorg. Chem.* **1999**, 1291.

(18) Koide, Y.; Barron, A. R. *Organometallics* **1995**, *14*, 4026.

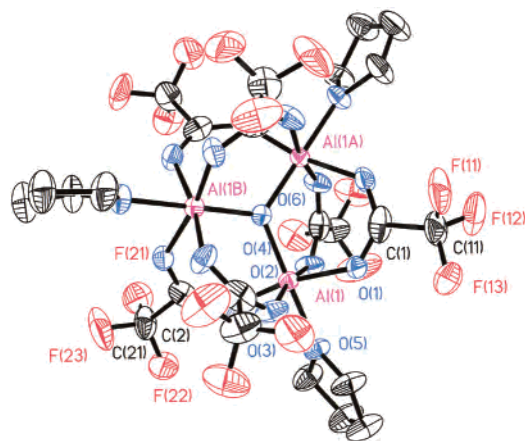


Figure 1. ORTEP plot of the non-hydrogen atoms of the cation of **3** (50% probability thermal ellipsoids). Selected bond lengths (Å) and angles (deg): Al(1)–O(1) 1.890(3), Al(1)–O(3) 1.895(3), Al(1)–O(5) 1.948(3), Al(1)–O(6) 1.8529(11), O(1)–C(1) 1.235(5), O(2)–C(2) 1.232(4), O(1)–Al(1)–O(2) 168.95(13), O(1)–Al(1)–O(5) 84.16(12), O(1)–Al(1)–O(6) 95.27(13), C(1)–O(1)–Al(1) 131.5(3).

cm^{-1} , the experimental 663 and 735 cm^{-1} bands were assigned to out-of-plane vibrations of the central oxo ligand.

Structure of $[\text{Al}_3(\mu_3\text{-O})(\mu\text{-O}_2\text{CCF}_3)_6(\text{THF})_3][(\text{Me}_3\text{Si})_3\text{CAl}(\text{O}_2\text{CCF}_3)_3]\cdot\text{C}_7\text{H}_8$. The molecular structure of the complex cation is shown in Figure 1. The central Al_3O core consists of a planar triangular arrangement of aluminum atoms (120°). Each aluminum atom possesses a slightly distorted octahedral coordination sphere. The $\text{Al}-(\mu_3\text{-O})$ distances in **3** (1.8529–11 Å) are longer than those in $\text{Pb}_2\text{Al}_5(\mu_3\text{-O})(\mu_4\text{-O})(\mu\text{-O}i\text{Pr})_9(\text{O}i\text{Pr})_3(\mu\text{-OAc})_3$ ($\text{Al}-(\mu_3\text{-O})$ 1.822 Å).¹⁷ The $\text{Al}-\text{O}$ (carboxylate) distances (av 1.892 Å) are comparable to those in analogous compounds¹⁸ ($\text{Al}-\text{O}(\text{carboxylate})$, av 1.892 Å) and smaller than the $\text{Al}-\text{O}$ (THF) bond lengths (1.948(3) Å) in **3**. The computed¹⁹ energy between the two possible conformations of the CF_3 groups obeying D_{3h} symmetry was estimated to be about 0.65 kcal/mol. This explains the rotational disorder detected in the X-ray crystal structure. The coordination sphere at the aluminum metal in the anion has a slightly distorted tetrahedral environment (Figure 2, $\text{Al}-\text{O}$ 1.784(3) Å). The cation and the anion molecular species possess trigonal elements, allowing quite high symmetrical packing within a rhombohedral space group ($R\bar{3}$). In the cation, three of the CF_3 groups are more disordered than the remaining ones. Including also the three CF_3COO^- groups of the anion, the 1:1:1 ratio of the resonances in the ^{19}F NMR is in line with the crystal

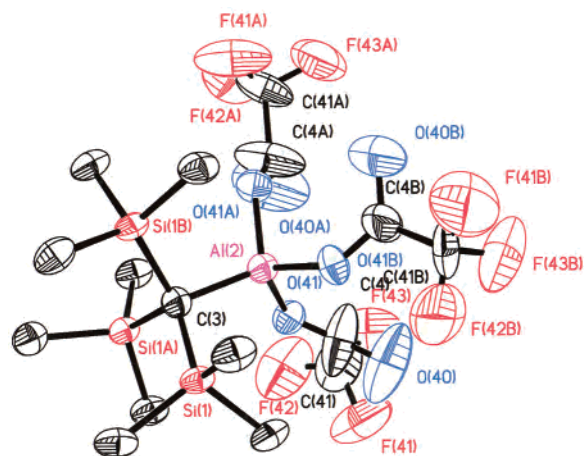


Figure 2. ORTEP plot of the non-hydrogen atoms of the anion of **3** (50% probability thermal ellipsoids). Selected bond lengths (Å) and angles (deg): Al(2)–C(3) 1.959 (7), Al(2)–O(41) 1.784(3), O(41)–Al(2)–C(3) 112.66(12), O(41)–Al(2)–O(41)#1 106.11(13).

structure, corresponding to the three different species of the carboxylate ligand. Moreover, two resonances are very close to each other, corresponding to the slightly differently arranged ligands in the complex cation.

Electronic Structural Analysis of Coordination Effects.

Compound **3** offers an interesting insight into the internal structural factors of the oxo-centered trinuclear core. The Al^{3+} , as a light and diamagnetic ion, is an excellent case study, where the coordination bonds of carboxylate and oxo ligands can be analyzed free of unpaired electrons, compared to transition metal ions. DFT calculations were performed¹⁹ for the $[\text{Al}_3(\mu_3\text{-O})(\mu\text{-OOCF}_3)_6(\text{H}_2\text{O})_3]^+$ cation, optimized under D_{3h} symmetry, considering water instead of THF as a ligand. The experimental symmetry is C_3 , but the coordination skeleton is very close to D_{3h} . The computed molecular geometry is in excellent agreement with the experimental one, even in the limits of idealized symmetry and without including the Madelung field in the calculation. For instance, the computed bond lengths, $\mu_3\text{-Al}-\text{O}$, 1.855 Å, and $\text{Al}-\text{O}$, 1.918 Å (carboxylate), can be compared with the experimental ones (given previously in this work). The $\text{O}-\text{C}-\text{O}$ and $\text{O}-\text{Al}-\text{C}$ bond angles are computed to be 127.3° and 131.1° , very close to the experimental values of 127.3° and 131.0° , respectively.

The structure of **3** shows the coordinated THF molecules in quasiplanar twisted conformations, with the mean planes perpendicular to those of the Al_3O fragment. Simulating the role of orientation of the terminal ligand by calculation with water as a ligand in the horizontal or perpendicular plane, it is found that the latter conformation is a bit more stable (~ 6 kcal/mol) than that with coordinated THF. The explanation can be found in the so-called metriotic principle,²⁰ stating that the arrangements using all the orbitals as much as possible in interatomic interactions are preferred against those configurations where only some of them are involved. In this view, the case with outer ligands perpendicular to σ_h is distributing more uniformly the π effects along the $\text{O}-\text{Al}-\text{O}$

(19) The calculations (including vibration frequencies) are based on B3LYP functional and 6-311G*, performed with Gaussian 98, Revision A.6. Frisch, M. J.; Trucks, G. W.; Schlegel, H. B.; Scuseria, G. E.; Robb, M. A.; Cheeseman, J. R.; Zakrzewski, V. G.; Montgomery, J. A., Jr.; Stratmann, R. E.; Burant, J. C.; Dapprich, S.; Millam, J. M.; Daniels, A. D.; Kudin, K. N.; Strain, M. C.; Farkas, O.; Tomasi, J.; Barone, V.; Cossi, M.; Cammi, R.; Mennucci, B.; Pomelli, C.; Adamo, C.; Clifford, S.; Ochterski, J.; Petersson, G. A.; Ayala, P. Y.; Cui, Q.; Morokuma, K.; Malick, D. K.; Rabuck, A. D.; Raghavachari, K.; Foresman, J. B.; Cioslowski, J.; Ortiz, J. V.; Stefanov, B. B.; Liu, G.; Liashenko, A.; Piskorz, P.; Komaromi, I.; Gomperts, R.; Martin, R. L.; Fox, D. J.; Keith, T.; Al-Laham, M. A.; Peng, C. Y.; Nanayakkara, A.; Gonzalez, C.; Challacombe, M.; Gill, P. M. W.; Johnson, B.; Chen, W.; Wong, M. W.; Andres, J. L.; Gonzalez, C.; Head-Gordon, M.; Replogle, E. S.; Pople, J. A. *Gaussian 98*, revision A.6; Gaussian, Inc.: Pittsburgh, PA, 1998.

(20) (a) Burdett, J. K. *Struct. Bonding (Berlin)* **1987**, 65, 29–90. (b) Burdett, J. K. *Molecular Shapes*; Wiley-Interscience: New York, 1980.

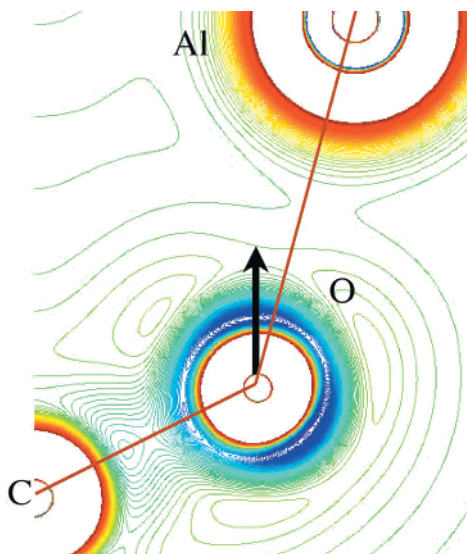


Figure 3. Laplacian of electron density in the plane of one carboxylate ligand. The blue areas identify the lone pairs of oxygen. The red-yellow zones mark the depletion of electron density, corresponding to ionized Al atoms. The arrows at O centers indicate the deviation of the maximal density of lone pairs from the Al–O axis. The bond path for Al–O (black solid line) is slightly curved inside. The blue diamonds mark the (3,–1) critical points of the Al–O bonds.

axis. Consequently, the metal centers devote different d orbitals to the interaction with the H₂O and the oxo ligands.

A quite surprising feature was the finding of slightly misdirected lone pairs between carboxylates and aluminum atoms. This feature is illustrated by the density map of Laplacian,²¹ (see Figure 3) in the coordination plane of one ligand, where the dark (blue) areas are showing the accumulation of electron density. The zones corresponding to the lone pair are deviating from the direction of the Al–O axis, being oriented inside of the C–O–Al triangle. Additionally, the lone pairs are deviating from the direction of the bond path, which is itself slightly curved inside.

In principle, a structural solution to regain the full orientation would be the reduction of the distance between the metal ions and the central oxygen. The Al–O distance from the anion shows that smaller bond lengths are possible. Such shortening will imply an increased pyramidalization (toward the central oxygen) of the metal centers with respect to the equatorial plane formed by the carboxylate oxygen donors. The factor preventing such an arrangement seems to be the preference for almost regular octahedral angles at aluminum. The slightly misdirected lone pair density is the result of opposite tendencies in a fine balance of small energy effects.

(21) (a) Bader, R. F. W. *Atoms in Molecules - A Quantum Theory*; Oxford University Press: Oxford, 1990. (b) Bader, R. F. W. *Acc. Chem. Res.* **1985**, *18*, 9–15. The AIMPAC code was used for present calculations.

The bond critical points are close to the metal ion, showing that the minimum of electron density along the bond axis practically occurs in the valence shell of the metal, as an expression of their positively ionized status. The light (orange) contours in Figure 3 are probing the general depletion of density around the aluminum centers (positive Laplacian).

The ionic bonding is also revealed through the natural bond orbitals analysis (NBO)²² that is correct for all the Al–O interactions (including π type) with $\sim 95\%$ ligand character, while, in the counterpart, the antibonding states have preponderant metal character (ligand field regime). The NBO analysis shows also the participation of the d orbitals in the natural hybrids of the Al centers, which are essential for the octahedral coordination. According to NBO results, and in full agreement with chemical intuition, the oxo ligand can be characterized using sp^2 hybrids. The central p_z is retrieved as a significant component of the HOMO orbital of the whole complex. The coordination strength of the ligands as it results from the bond order values can be arranged in the following order: (μ_3 -oxo) > carboxylate > terminal ligand.

Like the higher congeners (μ_4 -oxo-tetranuclears), the μ_3 -oxo-trinuclear species can be thought of as “inverse” coordination compounds, where the positive ions are surrounding and stabilizing a negative anion. The electronegativity and hardness of the oxygen is possibly the reason for the μ_3 -oxo-trinuclear arrangement. As a matter of fact, the μ_3 -oxo-trinuclear patterns appear only in connection with the transition metal elements in relatively high oxidation states, (III, IV) (when the metal ions are acquiring hard acid character). From this point of view, irrespective of the metal ion electronic configurations, the bonding within the μ_3 -oxo-trinuclear pattern can be characterized as driven by HSAB (hard and soft acids and bases) reasons and stabilized by the symmetric packing of the carboxylates.

Acknowledgment. M.F. is grateful to the Alexander von Humboldt Foundation for a research fellowship. The financial support of the Deutsche Forschungsgemeinschaft is acknowledged. We are grateful to Dr. N. Drago for technical assistance in using Gaussian 98.

Supporting Information Available: Tables listing detailed crystallographic data, atomic positional parameters, and bond lengths and angles. This material is available free of charge via the Internet at <http://pubs.acs.org>.

IC010880Y

(22) Reed, A. E.; Curtiss, L. A.; Weinhold, F. *Chem. Rev.* **1988**, *88*, 899–926. Glendening, E. D.; Reed, A. E.; Carpenter, J. E.; Weinhold, F. *NBO3.0 program*; University of Wisconsin, Madison. The NBO analysis was possible only for b3lypwave functions based on 3-21G* basis.